



Original Research Article

A Novel Study in the Determination of Loratadine in Pharmaceutical Samples by Precipitating with 3,5-Dinitrosalicylic Acid Utilizing the NAG_4SX3_3D Analyzer at 0-180° in Conjunction with the Continuous Flow Injection Analysis (CFIA) Technique

Issam Mohammad Shakir , Bakr Sadiq Mohammed* , Nagham Shakir Turkey 

College of Science, Chemistry Department, University of Baghdad, Republic of Iraq

ARTICLE INFO

Article history

Submitted: 07 November 2023

Revised: 03 December 2023

Accepted: 26 January 2024

Available online: 28 January 2024

Manuscript ID: [AJCA-2312-1462](https://doi.org/10.48309/AJCA.2024.429274.1462)

Checked for Plagiarism: **Yes**

Language editor:

[Dr. Fatimah Ramezani](#)

Editor who approved publication:

[Dr. Sami Sajjadifar](#)

DOI: [10.48309/AJCA.2024.429274.1462](https://doi.org/10.48309/AJCA.2024.429274.1462)

KEYWORDS

Loratadine

Continuous flow injection analysis (CFIA)

NAG_4SX3_3D analyzer

ABSTRACT

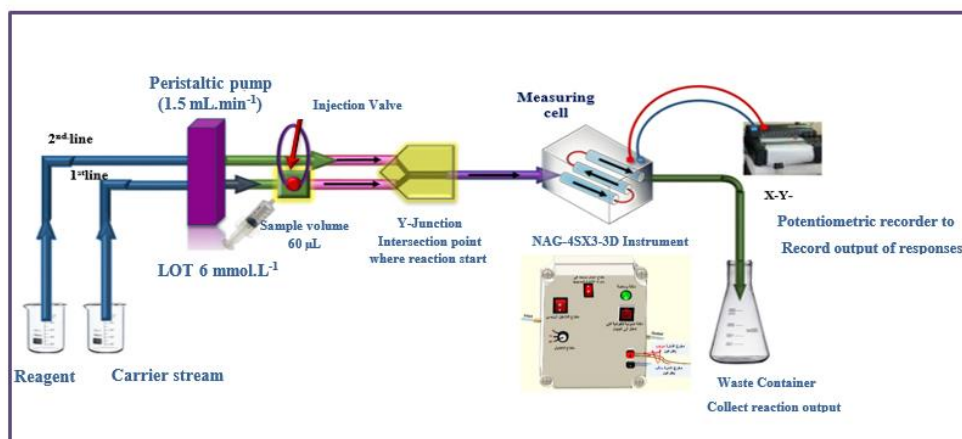
An innovative and effective method for continuous flow injection analysis (CFIA) was developed and included in the NAG_4SX3_3D Analyzer. The primary objective of this approach was to quantify the concentration of loratadine. This study presents a methodology for the quantification of loratadine, an antihistaminic medication, in pharmaceutical formulations. The samples are analyzed using the NAG_4SX3_3D Analyzer, which is a device that combines optical, chemical, electronic, and detection capabilities. The analyzer operates by receiving a cumulative signal, eliminating the need for amplification. The total distance travelled is 760 mm in relation to the variable Y_z -mV during a period of time represented by t seconds (measured in mm). The selection was made based on the accurate computation of the energy transducer profile. The relative standard deviations for loratadine are 0.09% at a concentration of 5 m.M and 0.1% at a concentration of 8 m.M for $n = 6$. The limit of detection (LOD) and limit of quantification were found to be 611.076 ng and 129 μ g, respectively, using a stepwise dilution of the lowest concentration on the calibration curve with a sample size of $n = 13$. The linear range has a correlation coefficient (r) of 0.9989, indicating a strong positive relationship. Additionally, the linearity of this range is measured at 99.79% (R^2) and recovery is not less than 96.58%, suggesting a high degree of conformity to a linear model. A comparative analysis was conducted between the outcomes of the suggested methodology and the existing UV-spectrophotometric approach, specifically at a wavelength of 275nm, revealing similar findings.

* Corresponding author: Sadiq Mohammed, Bakr

✉ E-mail: bakralalazaw98@gmail.com

© 2024 by SPC (Sami Publishing Company)

GRAPHICAL ABSTRACT



Introduction

Pharmacological intervention is the primary approach for managing allergies, with a significant number of individuals resorting to non-prescription antihistamines to alleviate symptoms of seasonal allergic rhinitis. Loratadine, marketed as Claritin, is a second-generation antihistamine used to treat the symptoms of allergic rhinitis and chronic idiopathic urticaria. It is known for its lack of sedative and anticholinergic effects, which have no substantial impact on clinical outcomes [1]. The compound may be identified by its chemical structure as 4-(8-chloro-5,6-dihydro-11H-benzo [5,6] cyclohepta[1,2-b] pyridine-11-ylidene)-1-piperidinecarboxylic acid ethyl ester. Therefore, it falls into the category of tricyclic selective blockers that target peripheral H₁-histamine receptors [2]. Loratadine has the chemical formula C₂₂H₂₃ClN₂O₂ with a molecular weight of 382.88 g/mol. Loratadine is often used for many applications. The primary applications of loratadine include: Allergic rhinitis therapy, hay fever treatment, alleviating sneezing and mitigating inflammation in the eyes and nose, a very efficient remedy for skin allergies, such as urticaria. Precautions was consider while using Loratadine throughout the pregnancy period. Topics of interest include breastfeeding, infant

care, geriatrics, and driving skills. The potential adverse reactions of loratadine include headache, fever, skin rash, gastrointestinal disturbance, and stomach discomfort [3]. Since the estimator is based on the use of a light-emitting diode, there are several techniques that are based on the use of a light-emitting diode as sources of incident light, many of which rely on continuous flow injection analysis [4-11]. There are some techniques that have been used to estimate allergen inhibitors such us AFM [12,13] and NAG Dual & Solo (0-180°) analyzer [14]. Loratadine has been determined in pure and pharmaceutical forms using a number of techniques, such as HPLC [1,15-17], LC/MS/MS [17-21], Cathodic stripping voltammetry (CSV) [22], UV-Spectrophotometric, and X-ray photoelectron spectroscopy [23-26]. This study gives the first results on how to use the newly created home-made NAG_4SX3_3D Analyzer [27], which has four sources of white snow LEDs set up in three rows, each corresponding to three detectors, which is a device that combines optical, chemical, electronic, and detection capabilities.

The analyzer operates by receiving a cumulative signal, eliminating the need for amplification. The total distance travelled is 760 mm in relation to the variable Y_z -mV during a period of time represented by t seconds (measured in mm). The selection was made based on the accurate

computation of the energy transducer profile, to measure the amount of loratadine in turbidimetric samples using flow analysis. Therefore, a small and inexpensive optoelectronic detector was made to provide accurate turbidimetric measurements in the context of continuous flow injection analysis, and a noticeable white precipitate was created. The amount of loratadine was measured by observing how they mixed 3,5-dinitro salicylic acid. Using a uniquely developed NAG_4SX3_3D Analyzer, the precipitate result was examined at 0-180°.

Experimental

Materials and methods

Chemical preparation

All of the materials and substances used in this investigation were of analytical grade, unless explicitly stated differently. Loratadine with a concentration of 0.02 M has been prepared by weighing 3.8288 g and dissolving in 500 ml of methanol, and the reagent 3,5-dinitro salicylic acid with a concentration of 0.05 M has been prepared by weighing 1.1406 g and dissolving in 100 ml of water.

Apparatus

The signal obtained from the reduction of light (0-180°) is depicted in Figure 1.A. This signal is acquired using a flow chamber that has been constructed using an internally assembled NAG_4SX3_3D Analyzer. The potentiometric recorders utilized for recording output signals are produced by Siemens, a renowned German company. A Teflon sample loop, equipped with six ports, is interconnected with a peristaltic pump that possesses adjustable length. The UV spectrophotometric device produced by Shimadzu, a renowned manufacturer based in Japan, was employed to carry out the standard procedures.

Methodology

According to the information presented in Figure 1 (A), the procedure for quantifying loratadine (LOT) involves the utilization of 3,5-dinitrosalicylic acid (DNSA) to produce a white precipitate[28]. The manifold of the NAG_4SX3_3D Analyzer comprises two interconnected lines. The system incorporates a sample segment introduction device, which consists of an injection valve with load and injection locations. This device enables the consistent and reliable administration of a predetermined quantity through repetitive injections. The flow rate of the NAG_4SX3_3D Analyzer is determined to be 1.5 milliliters per minute.

The system is linked to a Y-junction point, through which the sample zones of the lot are conveyed via a conveyor line that is supplied by the first line. The conveyance line, responsible for transporting the LOT sample zones at a concentration of 6 mM, is constructed using distilled water. The volume of the sample introduced is 60 microliters (μL). The study involved the analysis of the transducer's energetic response to sedimentary species and the assessment of light attenuation on the surfaces of white precipitate using an x-y potentiometric record output.

The examination of each solution was conducted in three replications. Scheme-1 proposes the precipitation of LOT 6 m.M using 4.0 m.M of DNSA. Figure 1(B) illustrates the progressive measurements of the NAG_4SX3_3D Analyzer transducer output (Yzi in millivolts) in relation to t.min (in decimal millimeters) for LOT concentrations of 6 millimolar. The LOT-DNSA system demonstrates clear and coherent outputs that are synchronized and legibly displayed. The NAG_4SX3_3D analyzer incorporates a novel synchronization strategy.

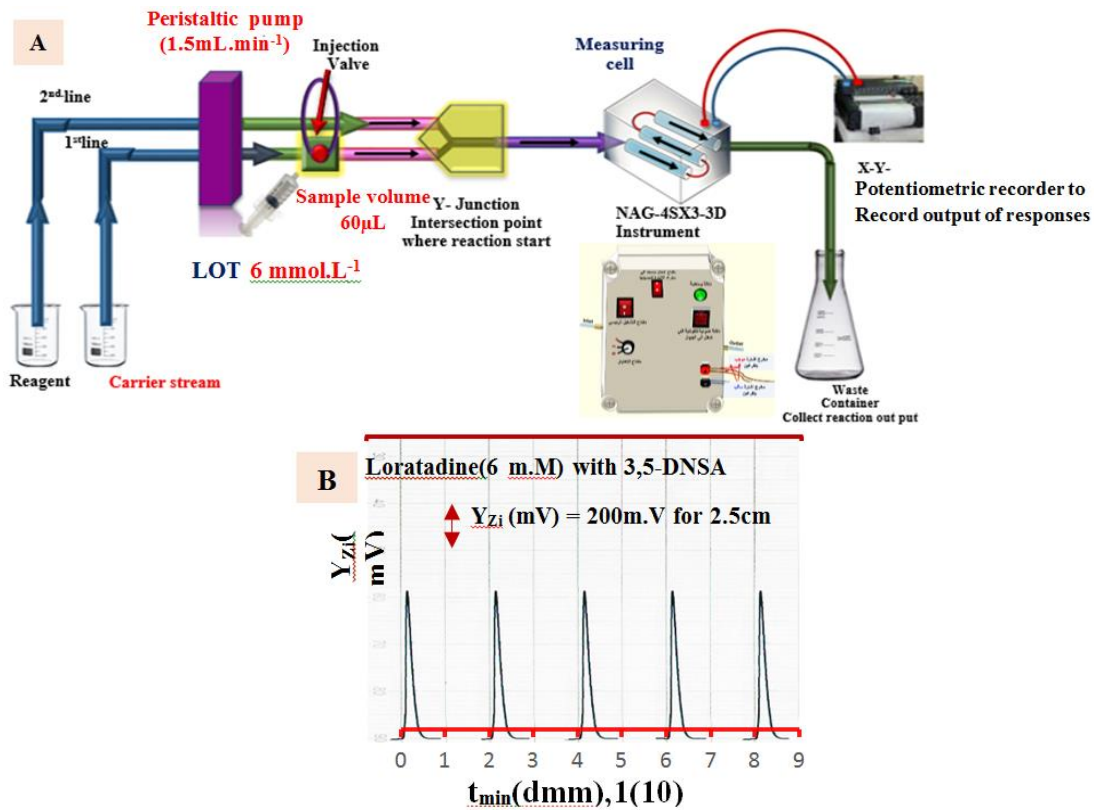
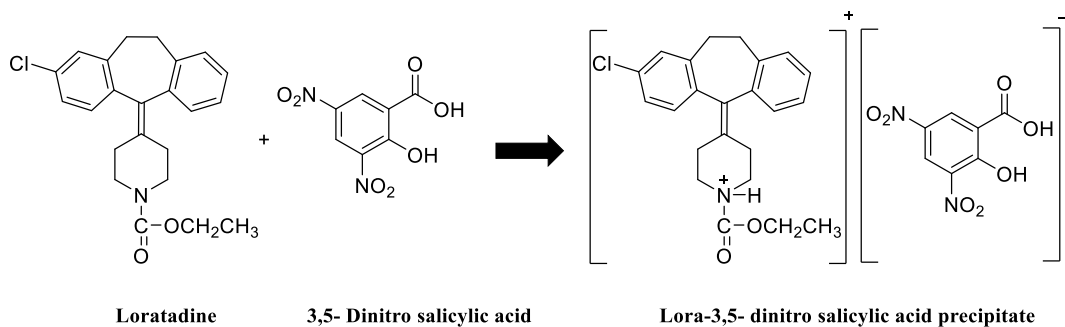


Figure 1. (A) Utilization of manifold in the evaluation of the NAG_4SX3_3D Analyzer **(B)** Initial and replicated examinations using the reaction of loratadine (6 m.M) with 3, 5 dinitro salicylic acid to produce a white precipitate for the evaluation of the NAG_4SX3_3D instrument.



Scheme 1. Proposed reaction for LOT – 3,5-DNSA- system[28].

Results and Discussion

Chemical parameters

3,5-dinitro salicylic acid

A series of 3,5-DNSA solutions with concentrations ranging from 1.0 to 10.0 m.M. were created by diluting an initial stocking

solution with distilled water. The experimental methodology included the use of a 60 µL sample volume. The reagent and carry line flow rates were 1.5 mL/min. The carry line contained distilled water. The experimental procedure entailed the tripartite replication of each measurement. Throughout this study, we use a NAG_4SX3_3D Analyzer to examine how changes

in 3,5-DNSA concentrations affect the energy transducer response.

Figure 2 (A) provides an illustration of this concept. The investigations discovered that the precipitated species in the LOT 6 m.M-3,5-DNSA system demonstrated a higher level of reactivity as the concentration of 3,5-DNSA increased, reaching a maximum at 4 m.M. Nevertheless, peak height was reduced and peak base width (Δt_B) was increased when concentrations

exceeded 4 m.M. The optimal concentration of 3,5-DNSA was found to be 4.0 m.M. in further studies; the greatest height of the peak and a meaningful response profile were obtained at this concentration. The system's output is shown in Table 1 (A) and Figure 2 (B), whereas Tables 1 (B) presents the segmentation technique that was used to choose the best portion. The ideal range for the LOT 6 m.M- 3,5-DNSA system are segments S_2 (3.0-6.0 m.M).

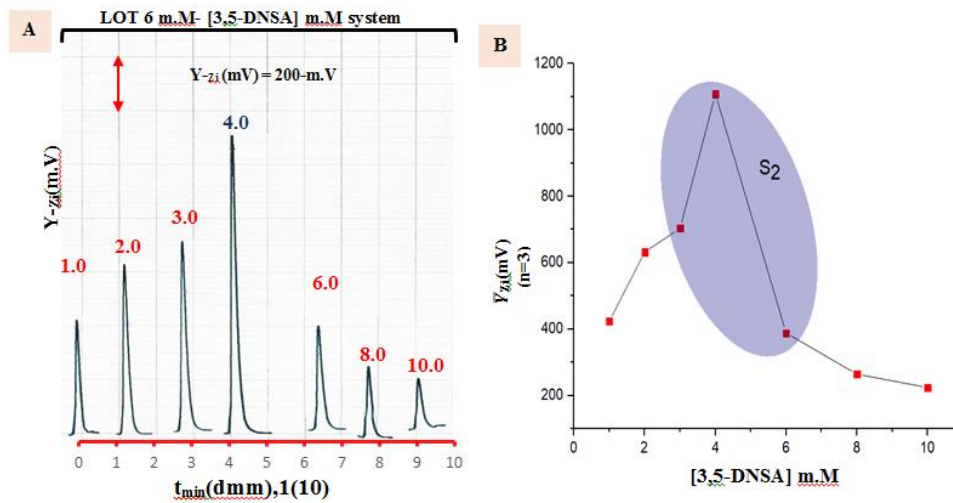


Figure 2. (A) Effect of 3,5-DNSA concentrations on the response-profile. (B) \bar{Y}_{-z_i} (m.V). The analysis comprises a set of three data points, which are regarded as a single segment, together with the determination of the most advantageous choice.

Table 1. (A) Effect of 3,5-DNSA concentrations on precipitation of loratadine in two systems and (B) Segmentation pattern: a (intercept m.V), b (slope m.V/ m.M), r (correlation coefficient), and θ (angle) with selection of optimum segment

A					
[m.M] of [3,5-DNSA] Reagent	\bar{Y}_{-z_i} (n:3)	R.S.D(%)	C.I at 0.05		
			\bar{Y}_{-z_i} (m.V) \pm t. σ_{n-1} / \sqrt{n}		
1	424	0.29	424 \pm 3.006		
2	632	0.22	632 \pm 3.428		
3	704	0.18	704 \pm 3.230		
4	1108	0.11	1108 \pm 3.056		
6	388	0.31	388 \pm 3.031		
8	264	0.47	264 \pm 3.080		
10	224	0.69	224 \pm 3.826		
B					
Segment	Reagent range m.M	(a)	(b)	(r)	(θ)
S ₁	1 -3	306.66	140.00	0.9629	89.591
S ₂	3 - 6	1347.43	-141.71	-0.5998	-89.598
S ₃	6 - 10	620	-41.00	-0.9589	88.603

\bar{Y}_{-z_i} (m.V):(S/N)- responses of NAG_4SX3_3D Analyzer in m.V((S/N)-R.N.A), $t_{0.025,2}=4.303$, SEM= Standard error of mean.

Effect of aqueous salts and acids solutions

The reactions between loratadine (6 m.M) and DNSA utilized distilled water (aqueous medium) as a carrier stream. Therefore, other aqueous solutions ($\text{CH}_3\text{COONH}_4$, NH_4Cl , NaCl , Na_2SO_4 , Na_2SO_3 , KCl , KI , CH_3COOH , HCl , HNO_3 , H_2SO_4 , and H_3PO_4) were generated at a concentration of 100 m.M and used as a carrier stream in place of distilled water in order to investigate whether they may increase the S/N (energy transducer response). Throughout the experiment, the reagent line and carrier stream line were kept in

an open valve state, with a sample volume of 60 μl and a flow rate of 1.5 mL/min. It is observed that the response's sensitivity rises when various salts and acids are used as a carrier stream because the energy transducer response decreases. The dispersion of particle precipitate in the presence of acids and salts is responsible for the phenomena that have been reported. To get the maximum response, the aqueous medium was determined to be the ideal carrier stream. Table 2 presents an overview of the results gathered.

Table 2. Different media's effects on the LOT 6 m.M-[3,5-DNSA]-4.0 m.M, a white precipitate is produced

Medium type 100m.M		\bar{Y} -Zi m.V. (n=3)	R.S.D(%)	C.I at 0.05 \bar{Y} -Zi(m.V) \pm t σ n-1 / \sqrt{n}
1	H ₂ O	1108	0.12	1108 \pm 3.180
2	CH ₃ COONH ₄	16	6.13	16 \pm 2.435
3	NH ₄ Cl	388	0.50	388 \pm 4.795
4	NaCl	348	0.57	348 \pm 4.894
5	NaSO ₄	264	0.70	264 \pm 4.571
6	NaSO ₃	128	0.85	128 \pm 2.708
7	KCl	304	0.39	304 \pm 2.931
8	KI	412	0.32	412 \pm 3.279
9	CH ₃ COOH	948	0.20	948 \pm 4.670
10	HCl	68	0.56	68 \pm 0.944
11	HNO ₃	124	0.71	124 \pm 2.186
12	H ₂ SO ₄	152	0.55	152 \pm 2.087
13	H ₃ PO ₄	600	0.21	600 \pm 3.080

Physical variables

Flow rate

Using their respective optimum concentrations, the LOT (6 m.M)-DNSA (4.0 m.M) system was applied to a sample volume of 60 μL . 0.9 to 2.5 mL/min as a variable flow rate (F.R.) was used (Figure 3(A)). The obtained findings are shown in Table 3. It was shown that at lower flow rates, the peak response's maximum height deformation and base width (Δt_B) both increased. The dispersion factor rises as a consequence of diffusion. It was discovered that peak height decreased at flow rates greater than

1.5 mL/min. The decrease in the height of the response profile is due to dilution and dispersion. The study indicates that the ideal flow rate for the LOT (6 m.M)-DNSA (4.0 m.M) system is 1.5 mL/min. This indicates that a flow rate increase over 1.5 mL/min causes an irregular response because precipitated particles move more rapidly and may pass in front of the measurement cells faster. The slope-intercept approach calculates the optimal flow rate of the carrier stream inside the segment selected for the LOT (6 m.M)-DNSA system, which is S1 (0.9-1.3 mL/min), as demonstrated in Figure 3(B) and Table 3(B).

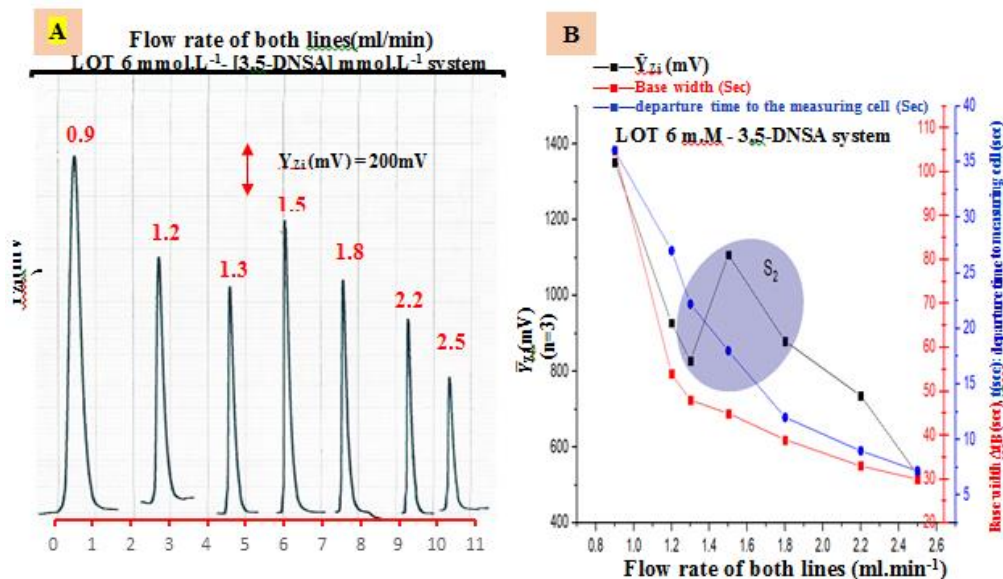


Figure 3. (A) Responses profile of flow-rate effect. **(B)** The output of the power a transducer response, denoted as $\bar{Y}_{Zi}(\text{m.V})$.The analysis includes three data points, which are considered as one segment, and the selection of the optimum choice.

Table 3. (A) Impact of flow rate

Pump speed (F.R) for each line	(F.R) mL/min	$\bar{Y}\text{-Zi}$ $n=3$	R.S.D(%)	C.I at 0.05 $\bar{Y}\text{-Zi}(\text{mV}) \pm t \sigma n-1 / \sqrt{n}$	Δt_B sec	V. (mL) at flow cell	C (m.M)	D	t sec
5	0.9	1352	0.15	1352±4.919	105	3.21	0.112	53.50	36.0
10	1.2	928	0.20	928±4.546	54	2.22	0.162	37.00	27.0
15	1.3	828	0.19	828±4.025	48	2.14	0.168	35.67	22.2
20	1.5	1108	0.14	1108±3.826	45	2.31	0.156	38.50	18
25	1.8	880	0.19	880±4.149	39	2.40	0.150	40.00	12
30	2.2	736	0.27	736±4.894	33	2.48	0.145	41.33	9
35	2.5	528	0.36	528±4.670	30	2.56	0.141	42.67	7.2

$\bar{Y}\text{-Zi}(\text{mV})$:(S/N) energy transducer response in m.V, $t_{0.025,2}=4.303$, Δt_B (sec) :Base width of peak (sec), t_{sec} : Departure time of sample segment out of injection valve reaching the flow tube, C : Concentration, D : Dilution factor at flow cell

Table 3.B: Segmentation pattern

Segment	F.R mL/min	(a)	(b)	(r)	(θ)
S1	0.9-1.3	2547.690	-1333.850	-0.9981	-89.957
S2	1.3-1.8	883.789	35.798	0.0605	88.400
S3	1.8-2.5	1787.459	-495.135	-0.9826	-89.884

Sample volume

The study utilized sample volumes (S.V) ranging from 25 μL to 326 μL . The volumes of the Teflon tubes used in this study varied in length from 3.18 cm to 41.5 cm, with a consistent diameter of 1 m.M. Figure 4 illustrates a gradual increase in

the attenuation of incident light (S/N profiles) up to 228 μL . Increasing the sample size leads to greater formation of precipitate particles which, in turn, leads to an increased height of the profile. A decline in the output response profile was noted when the volume surpassed 228 μL . The

presence of dense precipitate particles can impede the dispersion of all precipitated particles, leading to a decrease in the attenuation of incoming light. The 228 μL sample plug has been determined to be the most satisfactory based on analysis and slope-intercept calculation.

The conclusion is based on the findings from Tables 4 (A and B), which indicate that the ideal segment for the sample plug falls within the range of 228-326 μL for both. The optimal parameters can be determined by selecting a sample volume from the chosen segment.

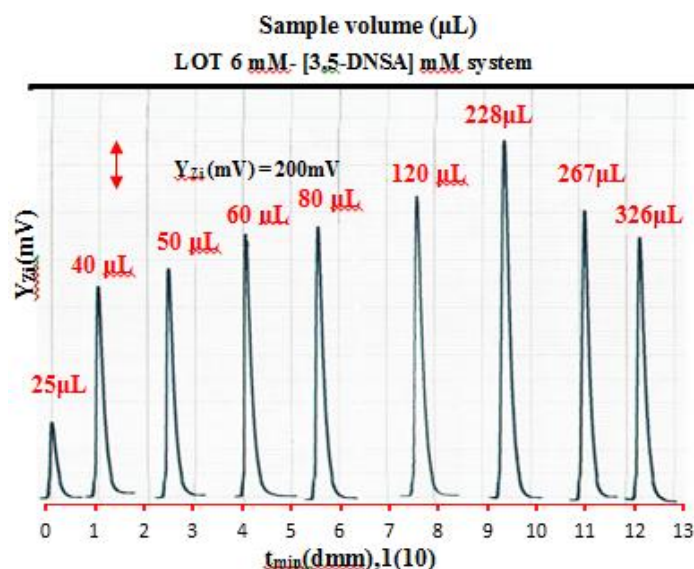


Figure 4. Responses-profile of sample volume (S.V).

Table 4. (A) Variation effect of (S.V) on formation of white precipitate

Length of (S.V) cm r= 0.5 mm	S.V μL	$\bar{Y}-Z_i$ ($n=3$)	R.S.D(%)	C.I.at 0.05		Δt_B sec	V. (mL) at flow cell	C (m.M)	D	t sec
				$\bar{Y}-Z_i(\text{mV}) \pm t. \sigma$	$n-1 / \sqrt{n}$					
3.18	25	324	0.38	324 ± 3.080	30.0	1.53	0.098	61.00	3.0	
5.10	40	888	0.18	888 ± 3.925	31.0	1.59	0.151	39.75	13.8	
6.37	50	960	0.19	960 ± 4.546	39.0	2.00	0.150	40.00	16.2	
7.64	60	1108	0.18	1108 ± 4.844	45.0	2.31	0.156	38.50	18.0	
10.20	80	1152	0.17	1152 ± 4.894	48.0	2.48	0.194	31.00	21.0	
15.30	120	1264	0.15	1264 ± 4.571	50.0	2.62	0.275	21.83	24.0	
29.00	228	1504	0.13	1504 ± 4.770	51.0	2.78	0.492	12.18	27.0	
34.0	267	1220	0.15	1220 ± 4.670	55.8	3.06	0.524	11.45	28.2	
41.5	326	1100	0.18	1100 ± 4.869	58.2	3.24	0.604	9.93	30.0	

Table 4. (B) Segmentation pattern

Segment	S.V (μL)	(a)	(b)	(r)	(θ)
S1	25-50	-288.000	26.400	0.9538	87.831
S2	60-120	946.857	2.629	0.9984	69.171
S3	228-326	2356.667	-3.954	-0.9402	-75.806

Effect of reaction loop lengths

To enhance the sensitivity of the reaction between loratadine and the reagent, efforts were made to increase the formation of precipitated particulate in the two-line manifold system. The study examined the LOT-DNSA system (6 m.M) using a F.R of 1.5 mL/min. The S.V used was 228 μ L. Each delay reaction coil was attached beyond the Y-junction point. To investigate the impact of mixing coil length on ion pair formation, it is necessary to determine the reaction completion time between LOT and reagent using a Teflon tube. The study investigated the optimization of a mixing coil by using Teflon tubes of varying

lengths (10, 20, 25, and 30 cm), corresponding to volumes of (314 μ L, 628 μ L, 785 μ L, and 942 μ L), respectively. The findings show that, in comparison to the system without a mixing coil, the peak height's sensitivity has increased (Figure 5). This implies that when a reaction coil with a length of 785 μ l is utilized, the reaction between LOT and DNSA is complete.

Therefore, the manifold system does not require a longer mixing coil. Figure 5(B) illustrates the utilization of the slope-intercept method to determine the optimal segmentation, segment S₂(628-942) μ L. All the results are summarized in Table 5 (A and B).

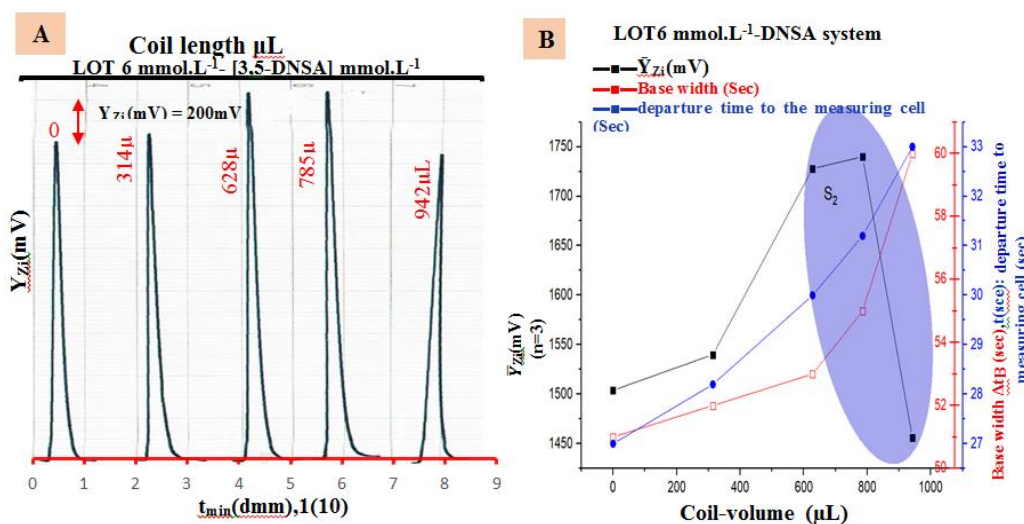


Figure 5. (A) Reaction coil responses profile, (B) \bar{Y}_{Zi} (m.V) out.put optimum choice.

Table 5. Finding of the impact of reaction coil, (B) Segmentation pattern

Coil length cm	Coil volume μ L	\bar{Y}_{Zi} ($\bar{n}=3$)	R.S.D(%)	C.l at 0.05 \bar{Y}_{Zi} (mV) $\pm t \sigma$ $n-1 / \sqrt{n}$	Δt_B sec	V.(mL) at flow cell	C (m.M)	D	t sec
Without	0	1504	0.130	1504 \pm 4.894	51.0	2.778	0.492	12.18	27.0
10	314	1540	0.128	1540 \pm 4.919	52.0	2.828	0.484	12.40	28.2
20	628	1728	0.122	1728 \pm 5.217	53.0	2.878	0.475	12.62	30.0
25	785	1740	0.107	1740 \pm 4.646	55.0	2.978	0.459	13.06	31.2
30	942	1456	0.143	1456 \pm 5.167	60.0	3.228	0.423	14.16	33.0
Segment	Coil volume (μ L)	(a)	(b)	(r)	(θ)				
S1	0-628	1478.667	0.357	0.9311	19.631				
S2	628-942	2321.333	-0.866	-0.8467	-40.900				

Analyzing the effect of converging chambers or points of intersection on the reaction pattern through the use of various designs

To make the critical process of solution mixing for the generation of precipitated particles easier, a variety of designs with varying capacities of mixing chambers have been used. Particle control and uniform distribution were evaluated by measuring various diameters before the particles entered the flow tube and were subjected to agglomeration. Finding the ideal conditions was the first step in conducting this experiment. All findings are summaries in Table 6, and Figure 6 displays the collected responses. This investigation produced a broad base and a

short peak height. Some reactions are not accurate. When reactants arrive to the measurement cell in a turbulent flow, it might be due to an incomplete reaction or non-homogeneous mixing of the complementary reactant in the huge mixing chamber. Its dispersibility is influenced by physical processes including dilution and dispersion, components that influence the distribution of precipitated particulate on the moving segment of the measurement cell. The analysis comes to the conclusion that a tube with an inner diameter of 2 m.M and an outer diameter of 4 m.M intersects at the ideal location to combine reactants to create precipitated particles, producing a volume of 12.56 μL .

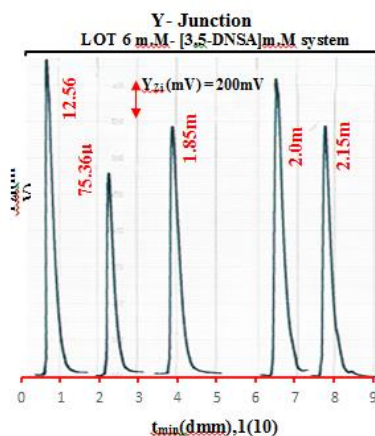


Figure 6. Response profile of Y_z (mV) - t_{min} (10m.M).

Table 6. The collected data set point for the determination process

Y-junction type		Volume $\pi r^2 h$	$\bar{Y}-Z_i(\bar{n}=3)$	tsec	V.mL At junction point	C (m.M) D
Intersection junction point	2 m.M (ID)(two inlet) 4m.M (length)(outlet)	12.56 μL^*	1740	31.2	1.788	0.765 7.84
	4 m.M (ID)(two inlet) 6 m.M (length) (outlet)	75.36 μL	1112	33.0	1.878	0.728 8.237
	14 m.M (ID) (outlet) 12 m.M(length)	1.85 mL	1360	34.2	1.938	0.706 8.50
	14 m.M (ID) (outlet) 13 m.M (length)	2.00 mL	1632	36.0	2.028	0.675 8.89
Premix chamber	14 m.M (ID) (outlet) 14 m.M (length)	2.15 mL	1376	40.8	2.268	0.603 9.950

t: Time.(Sec) from.injection.valve till the flow cell, C: Concentration before junction point or premix chamber, and D: Dilution factor, * optimum Y-junction

Determination of loratadine using NAG-4S3X-3D Analyzer and comparison with the classical methods

UV-Spectrophotometry method (reference method)

The UV-Vis spectrophotometric analysis was performed utilizing a 4.00 cm quartz cell and a Shimadzu model 1800 double-beam spectrophotometer. In Figure 7, the UV absorption spectra of the LOT are illustrated. A maximal absorbance of 275 nanometers was detected for the LOT [29], which was chosen as the maximum wavelength to calculate the working range, dynamic range, linear range, and scatter plot. With pure water, LOT concentrations between 0.05 and 9.0 m.M. were

created. After doing statistical computations, LOT discovered a linear range of 0.05-9.0 m.M., with a coefficient of determination (r^2) of 0.9965 and a correlation coefficient (r) of 0.9983. The dynamic range, working range, scatter plot, and linear range have all been identified. Table 7 displays the results of the regression line obtained by the UV-spectrophotometry method's statistical analysis.

Estimating a linear dynamical range for the impact of loratadine on the S/N energy transducer response using a scatter plot

In previous sections, the optimal values for the chemical and physical parameters for LOT were determined. The system's sample volume was 228 μ L with a delay reaction coil of 785 μ L and

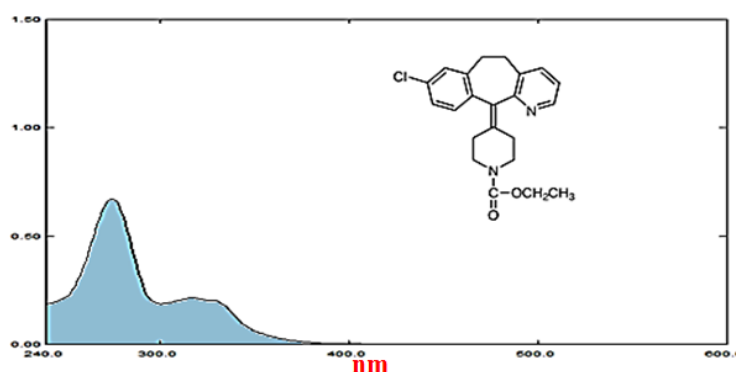


Figure 7. Absorbance of UV- Spectrum of loratadine at concentration of 3.0 m.M at λ_{\max} = 275 nm.

Table 7. The summary of statistical analysis of regression line of f reference method (UV spectrophotometry)

Type of mode	Range of [LOT] m.M (n)	$\hat{Y}_i = a \pm S_a + b(\Delta y / \Delta x \text{ m.Mol/L}) \pm S_b$ at confidence level 95%, n-2	r, r ² , R ² %	t tab at 0.05, n-2	Calculated t-value $t_{cal} = r / \sqrt{1-r^2}$
Linear range	0.05-7.0(24)	$0.024 \pm 0.027 + 0.271 \pm 0.007$ [LOT] m.M	0.9983, 0.9965, 99.65	2.074	$<< 79.992$
Working range	0.05-8.0(25)	$0.043 \pm 0.040 + 0.005 \pm 0.010$ [LOT] m.M	0.9961, 0.9922, 99.22	2.069	$<< 54.190$
Dynamic range	0.05-8.5(26)	$0.066 \pm 0.055 + 0.253 \pm 0.013$ [LOT] m.M	0.9928, 0.9857, 98.57	2.064	$<< 40.692$
Scatter plot	0.05-9.0(27)	$0.091 \pm 0.068 + 0.242 \pm 0.014$ [LOT] m.M	0.9888, 0.9776, 97.76	2.060	$<< 33.065$

n = number of measurements, \hat{Y}_i : estimated value without unit by spectrophotometric classical method, r : correlation coefficient, r^2 : coefficient of determination, $R^2\%$: (percentage capital R-squared): explained variation as a percentage / total variation, and $t_{tab} = t_{0.05/2, n-2}$

1.5 mL/min (F.R) for the reagent line and carrier stream as shown in Figure 8. Various solutions containing LOT in the LOT-DNSA system have been developed, ranging in concentration from 0.05 to 20 mM. Moreover, for each measurement, we took three measurements. Plotting the transducer energy response versus the loratadine concentration was done. Table 8 displays the findings, the result was a straight line graph between 0.05 and 20 m.M. A correlation coefficient will diminish and deviate from linearity over 20 m.M. This phenomenon's most probable source is a rise of particles in front of a detector, which may be related to radiation attenuation. In addition, the results show that, up to concentrations of 20, there is a clear correlation between the variables.

However, the straight direct connection shown in the calibration graph starts to gradually diverge as concentrations rise. This might be due to a rise in precipitated particulate matter and its capacity to create an interparticle gap that is rather stiff, blocking the detector from receiving the remaining light. The recently created approach for figuring out the LOT-DNSA (4.0 mM) system was compared to an established reference technique called UV-spectrophotometry. Table 8 indicates the data obtained using the NAG_4S3X_3D Analyzer.

Detection of limit (LOD)

Table 9 presents the use of three separate methodologies to ascertain the limit of detection of loratadine.

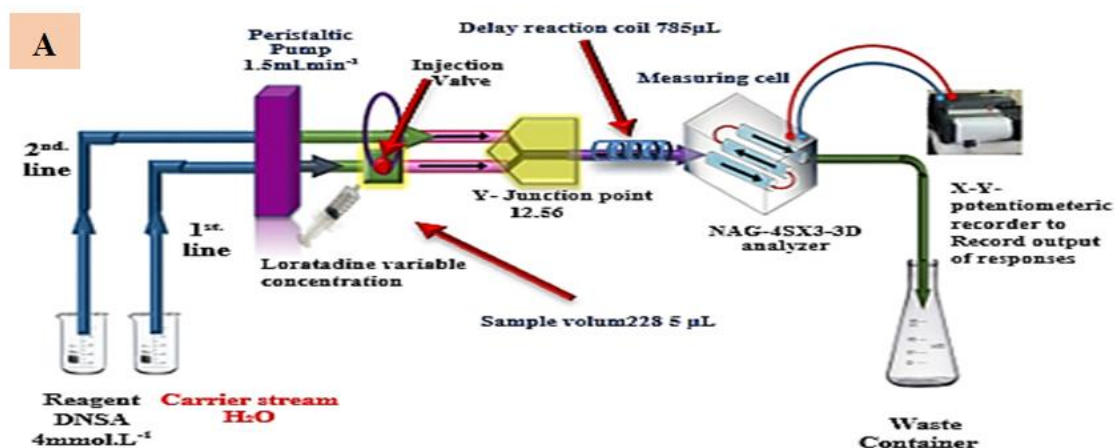


Figure 8. Determination of LOT using a flow gram technique in each system.

Table 8. Results of linear regression using a first-degree equation of the form =a+b x under ideal circumstances

Type of mode	Range of [Loratadine] m.M(n)	$\hat{Y}_i = a \pm Sa + b(\Delta y / \Delta x \text{ m.Mol/L}) \pm Sb$ [Loratadine] m.M at confidence level 95%, n-2	r, r2, R2%	t tab at 0.05, n-2	Calculated t-value $t_{cal} = r / \sqrt{1-r^2}$
Developed method using NAG - 4SX3 - 3D analyzer					
Linear range	0.05-9.0 (18)	$13.395 \pm 37.971 + 294.778 \pm 7.174$ [LOT] m.M	0.9989, 0.9979, 9.79	2.120	$<< 87.099$
Working range	0.05-10(19)	$18.718 \pm 38.233 + 292.823 \pm 6.782$ [LOT] m.M	0.9990, 0.9980, 9.80	2.110	$<< 76.405$
Dynamic range	0.05-15 (20)	$178.340 \pm 196.038 + 249.066 \pm 30.446$ [LOT] m.M	0.9709, 0.9426, 4.26	2.101	$<< 17.187$
Scatter plot	0.05-20(21)	$405.455 \pm 294.900 + 194.425 \pm 38.547$ [LOT] m.M	0.9243, 0.8544, 5.44	2.093	$<< 10.557$

n: no. of measurement, \hat{Y}_i (mV); estimated response(n=3) in mV for developed method and r: correlation coefficient, r²: coefficient of determination, and R²% (percentage capital R- squared): explained variation as a percentage/total variation and $t_{tab} = t_{0.05/2, n-2}$,

1. Gradual dilution: The dependability and significance of the detection limit (D.L.) are attributable to the gradual dilution of the minimal concentration observed in the scatter plot.

2. Theoretically: The calculation depends on the dynamic range and the slope method.

3. Theoretically: The selection of a method is influenced by the linear dynamic range, which is determined by the low residual value ($S_{y/x}$), also known as S_b in the equation $\hat{Y} = Y_b + 3S_b$, where Y_b represents the A_v response regarding the missing solution. The variable "a" in the linear equation $y = a + bx$ represents the intercept [30,31].

Repeatability

The evaluation of the accuracy that the whole assay process achieved, as shown in Table 10, consists of the combination of measurements that were taken for two distinct LOT-DNSA system concentrations. Every measurement was made six times in a row. The information shows

that the RSD% was below 0.11% of the concentration [32].

Determination of Loratadine in drugs using a homemade NAG_4SX3_3D analyzer

By employing the NAG-4SX3-3D analyzer and comparing the results with the classical spectrophotometric method based on the measurement of λ_{max} at 275 nm [29]. The proven technique was utilized to determine LOT in four distinct types of LOT samples obtained from four renowned pharmaceutical manufacturers: (Lartin, 10 mg, WADI ALRAFIDAIN, Iraq); (Lorasam, 10mg, SDI, Iraq); (Lohist, 10mg, SAOG, Oman); and (Pressing, 10mg, Helmofarm, Serbia). The standard addition method was applied for the LOT-DNSA(4m.M) system by preparing series of solutions from each pharmaceutical drug (5 m.M-0.1914 gm of active ingredient in 100 mL) by transferring 0.5 mL to each of the five volumetric flask (10 mL), followed by the addition of gradual volumes of

Table 9. The detection limit of Loratadine for both systems was determined using an injection sample volume of 228 μ L and optimal parameters

Practically depending on the scatter plot's minimum concentration at a progressive dilution		Theoretical based on the value of slope $x=3S_b/slope$	Theoretical based on the linear equation $\hat{Y} = Y_b + 3S_b$	Limit of quantitative L.O. Q $\hat{Y}=Y_b+10S_b$
Newly developed method (7) μ mo.L ⁻¹ for LOT -DNSA system	Classical method Uv-sp LOT -DNSA system			
611.076 ng/sample	19.144 μ g/ sample	1.073 μ g/sample	38.606 μ g/sample	0.129 ⁹ mg/sample

\hat{Y} : Estimated response (mV), X :value of LOD based on the slope(depend on linear dynamic range), S_b : standard deviation of blank($n=13$) equal to $S_{y/x}$ (residual), (LOD depend on linear equation of linear range due to low $S_{y/x}$), Y_b : A_v response for blank=intercept (a).

Table 10. Repeatability of Loratadine at optimum parameters with 228 μ L S.V

[Loratadine] m.M	\bar{Y}_{-z_i} (m.V) Av of responses (n=6)	R.S.D(%)	C.I at 0.05 \bar{Y}_{z_i} (mV) $\pm t_{0.05/2, \sigma_{n-1}} / \sqrt{n}$
LOT -DNSA (4 m.M) system			
5	1528	0.09	1528 \pm 1.394
8	2420	0.10	2420 \pm 2.448

$t_{0.05/2,5}=2.571$, n = number of injections

0.02 m.M standard of Loratadine (0, 0.5, 0.6, 0.7, and 0.8) mL for the LOT-DNSA (4 m.M) system which equivalent to : 0,1.0, 1.2, 1.4, and 1.6 m.M for NAG_4SX3_3D Analyzer, classical UV-Spectrophotometric method[29]. The study's response profile is shown in Figure 9. The findings of the standard additions method for the four samples including LOTs of pharmaceutical medicines are summarized in Table 11 (A). The findings for the two procedures are summarized in Table 11 (B). They include the t-test for comparison at two distinct pathways, the efficiency of determination, and the practical amount of the active component at a 95% confidence level [33].

Individual t-test [33]: Table 11 (B) presents a comparison between the newly established approach and the official stated value ($\mu_0=10$ mg) for Lartin (Iraq), Lorasam (Iraq), Lohist (Oman), and Pressing (Serbia). The following estimate of a hypothesis may be made using the determined tcal of each unique company:

H_0 (Null hypothesis): For sample no. 1: $\mu_0 = \bar{W}_1$ for Lartin - Iraq For sample no. 2: $\mu_0 = \bar{W}_2$ for Lorasam -Iraq For sample no. 3: $\mu_0 = \bar{W}_3$ for Lohist - Oman For sample no. 4: $\mu_0 = \bar{W}_4$ for Pressing -Serbia

That is the means of practical content for three distinct firms (W_i) do not significantly deviate from the reference value ($\mu_0 = 10$ mg) Against H_1 (alternative hypothesis): $\mu_0 \neq \bar{W}_i$ for four different companies

That is there appears to be an evident variation between the reported numerical values and the Av values of practical substance across four distinct companies.

Paired t-test [34]: An examination was conducted to evaluate the effectiveness of a developed method of analysis, using the NAG_4SX3_3D Analyzer, in comparison to traditional techniques as spectrophotometry. This study included analyzing four samples that were taken from different companies. It is critical to recognize that comparing various manufacturers may result in the possible disdain for individual variance.

A hypothesis can be estimated as a follow:

Null hypothesis H_0 : $\mu_{NAG_4SX3_3D \text{ analyzer}} = \mu_{UV-Spectrophotometric}$
 $\mu_{NAG_4SX3_3D \text{ analyzer}} = \text{official method}$
 Against
 Alternative hypothesis H_1 : $\mu_{NAG_4SX3_3D \text{ analyzer}} \neq \mu_{UV-Spectrophotometric}$
 $\mu_{NAG_4SX3_3D \text{ analyzer}} \neq \text{Official method}$

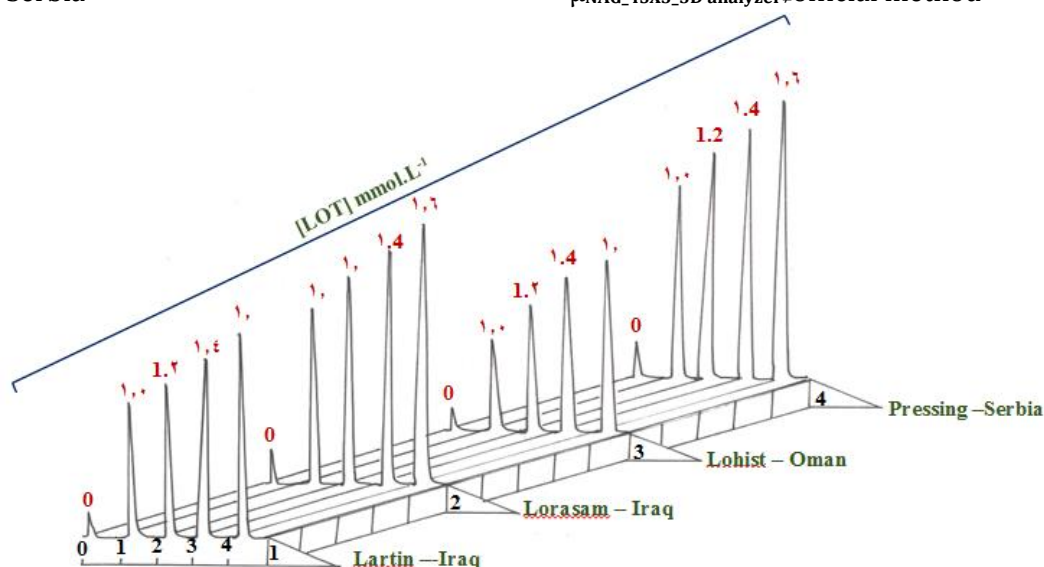


Figure 9. Profile – time for standard addition method using four different companies: Sample 1: Lartin -10 mg-Iraq/Sample 2: Lorasam -10 mg-Iraq/Sample 3: Lohist – 10 mg-Oman/Sample 4: Pressing -10 mg- Serbia.

Table 11. (A) Results of standard addition for the determination of LOT in four drug samples using the UV-Spectrophotometer technique (Classical method) and NAG - 4SX3 - 3D analyzer method

No. of sample	Commercial Name, Company Content, Country	Type of method					Equation of standard addition at 0.05 for n-2, r, r ² , R ² % $\hat{Y}_i(mV)=a\pm s_{at}+b\pm s_{bt}$ [LOT]m.Mol.L ¹ , r, r ² , R ² % $\hat{Y}_i=a\pm s_{at}+b\pm s_{bt}$ [LOT]m.M, r, r ² , R ² %
		NAG-4SX3-3D analyzer (mV)					
		UV- Spectrophotometer at $\lambda_{max}= 275nm$					
		LOT					
		0 mL	0.5 mL	0.6 mL	0.7 mL	0.8 mL	
		0	1.0	1.2	1.4	1.6	
1	(Lartin, WADI ALRAFIDAIN, 10 mg, Iraq	82	400	460	530	600	=79.938±14.685+321.598±12.480 [LOT]m.M 0.9998,0.9996,99.96 =0.081±0.053+0.328±0.045
		0.071	0.432	0.483	0.532	0.593	[LOT]m.M 0.9972,0.9945,99.45 =107.464±23.152+418.015±19.623
2	Lorasam, SDI, 10mg, Iraq	108	520	610	703	770	[LOT]m.M 0.9996,0.9993,99.93 =0.064±0.033+0.263±0.029
		0.064	0.321	0.393	0.421	0.489	[LOT]m.M 0.9983,0.9967,99.67 =68.402±31.594+274.613±26.700
3	Lohist, SAOG,10mg, Oman	65	355	390	400	500	[LOT]m.M 0.9986,0.9972,99.72 =0.055±0.051+0.223±0.045
		0.053	0.268	0.348	0.359	0.406	[LOT]m.M 0.9945,0.9891,98.91 =109.959±14.265+447.732±12.092
4	Pressing, Hemofarm ,10mg, Serbia	108	560	650	740	820	[LOT]m.M 0.9999,0.9998,99.98 0.087±0.029+0.348±0.024
		0.088	0.432	0.509	0.562	0.653	[LOT]m.M 0.9993,0.9986,99.86

\hat{Y}_{zi} : Estimated response in mV for developed method and without unite for UV-Sp. method, r: correlation coefficient, r²: coefficient of determination, R²% (percentage capital R- squared): explained variation as a percentage / total variation, $t_{tab} = \frac{t_{0.05}}{2}, \infty = 1.96$ at 0.05, $t_{tab} = t_{0.05/2,3} = 3.182$ for n=5, and UV-Sp.: UV-Spectrophotometric method, using volume of cell (quartz) 4 mL in UV-Spectrophotometric method

Table 11. (B) Summary of results for practical content, (Rec %) efficiency for determination of LOT in four samples of drugs and t-test for comparison two methods

No. of sample	Type of method NAG - 4SX3 - 3D Analyzer UV-Spectrophotometer at $\lambda_{max}= 275nm$. Weight of LOT in each sample(g) $\bar{W}_{i(g)} \pm 4.303 \sigma_{n-1} / \sqrt{n}$		Individual t-test between claimed value and practical value $(\bar{W}_{i(mg)} - \mu) / \sigma_{n-1}$	Paired t-test Compared between two method	
	Efficiency of determination Rec. % Weight of LOT in tablet $\bar{W}_{i(mg)} \pm 4.303 \sigma_{n-1} / \sqrt{n}$ (mg)	$t_{cal} = \frac{\bar{w}_d}{\sigma_{n-1}^*} / \sigma_{n-1}$		t_{tab} at 0.05 confidence level (n-1)	
1	0.1903 ± 0.0246	99.43	/-0.192 / < 4.303	Newly developed methodology and UV-spectrophotometric (classical method) for 1 st system $\bar{W}_d = -0.1012$ $\sigma_{n-1}^* = 0.1463$ /- 1.383 / < 3.182	
	9.9428 ± 1.283				
	0.1879 ± 0.0350	98.17	/-0.431 / < 4.303		
	9.8169 ± 1.826				
2	0.1891 ± 0.0254	98.77	0.920 < 4.303		
	9.8767 ± 1.325				
	0.1849 ± 0.0450	96.58	/-0.627 / < 4.303		
	9.6577 ± 2.348				
3	0.1907 ± 0.0351	99.63	/-0.086 / < 4.303		
	9.9634 ± 1.832				
	0.1875 ± 0.0370	97.93	/-0.461 / < 4.303		
	9.7929 ± 1.932				
4	0.1881 ± 0.0380	98.24	/-0.382 / < 4.303		
	9.8236 ± 1.987				
	0.1902 ± 0.0380	99.34	/-0.142 / < 4.303		
	9.9343 ± 1.987				

μ : claim value (10mg), \bar{w}_i : practically weight in mg, \bar{w}_d : Av weight of difference between two type of method (developed & classical), σ_{n-1} : standard deviation of different (paired t-test), n:(no. of sample) = 4, $t_{tab} = t_{0.05/2, n-1} = t_{0.025, 3} = 3.182$ (for individual t-test & paired t-test), and classical method: UV-Spectrophotometric method

Since calculation t_{cal} of $-1.383 / < 3.182$ at 0.05 confidence level. Therefore; H_0 is accepted against H_1 indicating that there is no significant difference between three methods.

Conclusion

The NAG_4SX3_3D Analyzer in conjunction with the continuous flow injection analysis approach is recommended, mended for examining loratadine because of its ease of use, quickness, affordability, and great sensitivity in both pharmaceutical and pure forms. When loratadine is precipitated with 3,5-DNSA, a white ion-pair product is produced.

By employing a linear array comprising twelve super-white light-emitting diodes as the light source and three solar cells as the detector, the precipitate is ascertained. It is assessed how much incoming light is attenuated at angles between 0° and 180°. Because it uses less costly reagents and equipment than spectrophotometry, the suggested approach is more affordable. A high degree of agreement was seen in all samples, indicating that the suggested method is precise enough. Reducing matrix effects was accomplished by using the traditional addition approach.

Orcid

Issam M. Shakir : [0009-0002-1810-3406](https://orcid.org/0009-0002-1810-3406)

Bakr S. Mohammed : [0009-0002-1784-1837](https://orcid.org/0009-0002-1784-1837)

Naghham Shakir Turkey : [0009-0002-7925-6633](https://orcid.org/0009-0002-7925-6633)

References

- [1] O.O. Mamina, V.I. Kabachny, N.Y. Bondarenko, O.V. Lozova, **2021**. [[Google Scholar](#)], [[Publisher](#)]
- [2] U. Matteredne, M.M. Böhmer, E. Weisshaar, A. Jupiter, B. Carter, C.J. Apfelbacher, *CDSR*, **2019**, [[CrossRef](#)], [[Google Scholar](#)], [[Publisher](#)]
- [3] R. Yamprasert, W. Chanvimalueng, N. Mukkasombut, A. Itharat, *BMC complement. med. ther.*, **2020**, *20*, 1-11. [[CrossRef](#)], [[Google Scholar](#)], [[Publisher](#)]
- [4] G.F. Hussein, *Int. J. Pharm. Res.*, **2021**, *13*. [[CrossRef](#)], [[Google Scholar](#)], [[Publisher](#)]
- [5] E.N. Mezaal, N.S. Turkey, *Int. J. Pharma. Res.*, **2019**, *11*, 42-57. [[CrossRef](#)], [[Google Scholar](#)], [[Publisher](#)]
- [6] A.H. Mhdi, S.S. Abed, *Chem. Methodol.*, **2023**, *7*, 435-446. [[CrossRef](#)], [[Publisher](#)]
- [7] N.S. Turkey, E.N. Mezaal, **2020**, *9*, 563-574. [[Google Scholar](#)]
- [8] N.S. Al Awadie, G. Khalid, *Int. J. Pharma. Res.*, **2021**, *13*. [[CrossRef](#)], [[Google Scholar](#)], [[Publisher](#)]
- [9] O.A. Yassin, N.S.T. Al Awadie, *Baghdad Sci. J.*, **2021**, *18*, 0565-0565. [[CrossRef](#)], [[Google Scholar](#)], [[Publisher](#)]
- [10] B.S. Mohammed, N.S. Turkey, *Chem. Pap.*, **2023**, 1-14. [[CrossRef](#)], [[Google Scholar](#)], [[Publisher](#)]
- [11] N.S. Turkie, S.F. Hameed, *Chem. Methodol.*, **2023**, *7*, 53-66. [[CrossRef](#)], [[Publisher](#)]
- [12] A.N. Jasim, N.S.T. Al-Awadi, *Sys. Rev. Pharm.*, **2020**, *11*. [[CrossRef](#)], [[Google Scholar](#)], [[Publisher](#)]
- [13] N.S.T. Al-Awadie, I.M.S. Al-Hashimi, K.H.I. Al-saadi, *Iraqi J. Sci.*, **2015**, *56*, 2745-2761. [[Google Scholar](#)], [[Publisher](#)]
- [14] J.N. Jeber, N.S. Turkey, *Int. J. Pharma. Res.*, **2020**, *12*, 2911-2924. [[CrossRef](#)], [[Google Scholar](#)], [[Publisher](#)]
- [15] M.M. Sebaay, N.I. Ziedan, *Curr. Drug Metab.*, **2019**, *20*, 1053-1059. [[CrossRef](#)], [[Google Scholar](#)], [[Publisher](#)]
- [16] N. AlMasoud, A.H. Bakheit, M.F.M. Alshammari, H.A. Abdel-Aziz, H. AlRabiah, *Profiles Drug Subst. Excip. Relat. Methodol.*, **2022**, *47*, 55-90. [[CrossRef](#)], [[Google Scholar](#)], [[Publisher](#)]
- [17] Q. Li, H.Y. Shi, K. Wang, M. Kan, Y. Zheng, G.X. Hao, X.M. Yang, Y.L. Yang, L.Q. Su, W. Zhao, *Curr. Pharm. Anal.*, **2020**, *16*, 909-915. [[CrossRef](#)], [[Google Scholar](#)], [[Publisher](#)]
- [18] Y. Zhang, J. Zhang, Q. Xu, Y. Wang, W. Wu, W. Wang, X. Li, T. Zhang, *Drug Des. Devel. Ther.*, **2021**, 5109-5122. [[CrossRef](#)], [[Google Scholar](#)], [[Publisher](#)]
- [19] Y. Zhang, Y. Lu, L. Wang, Y. Tian, Z. Zhang, *Drug Res.*, **2020**, *70*, 528-540. [[CrossRef](#)], [[Google Scholar](#)], [[Publisher](#)]
- [20] D. Yang, R. Li, C. Jia, F. Zhang, S. Jiang, P. Zhang, G. Ling, *Chromatographia*, **2020**, *83*, 183-190. [[CrossRef](#)], [[Google Scholar](#)], [[Publisher](#)]
- [21] N.S. Turkie, S.F. Hameed, *Chem. Methodol.*, **2022**, *6*, 731-749. [[Crossref](#)], [[Publisher](#)]
- [22] G. Önal, Y. Altunkaynak, A. Levent, *J. Iranian Chem. Soc.*, **2021**, *18*, 3465-3475. [[CrossRef](#)], [[Google Scholar](#)], [[Publisher](#)]
- [23] A. Ahmed Mohammed, S.H. Abdullah, G.H. Abdulwahhab, *Egyptian J. Chem.*, **2022**, *65*, 273-280. [[CrossRef](#)], [[Google Scholar](#)], [[Publisher](#)]
- [24] S.A. Rincón-Ortiz, A.C. García-Castro, R. Ospina, *Surf. Sci. Spectra*, **2022**, *29*. [[CrossRef](#)], [[Google Scholar](#)], [[Publisher](#)]
- [25] B. Prathap, M. Arivazhagan, S. Arikaran, R. Arthi, M. Arshad Khan, K. Balajeevarshan, S.

- Mohamed Halith, **2023**. [[CrossRef](#)], [[Google Scholar](#)], [[Publisher](#)]
- [26] H.M. Lotfy, S. El-Hanboushy, Y.M. Fayez, M. Abdelkawy, *Future J. Pharm. Sci.*, **2019**, 5, 1-14. [[CrossRef](#)], [[Google Scholar](#)], [[Publisher](#)]
- [27] IRQ-PATENT, NO. 6300, I.M.A. Shakir, N.S. Turkey, Novel Multiple Continuous Flow Cells (hydrophilic & hydrophobic) works as a Solo Flow cell with Summed S/N responses in NAG-4SX3-3D. 2020, Patent., International classification HO1J61/00, 2018.
- [28] A.I. Vogel, *London Longmans*, **1954**. [[Google Scholar](#)]
- [29] N. Jahan, I. Naveena, G. Madhusudhan, C.A. Kumar, N. Malathi, K. Soujanya, *Int. J. Pharm. Sci. Res.*, **2018**, 9, 65-73. [[Google Scholar](#)]
- [30] Á. Lavín, J.d. Vicente, M. Holgado, M.F. Laguna, R. Casquel, B. Santamaría, M.V. Maigler, A.L. Hernández, Y. Ramírez, *Sensors*, **2018**, 18, 2038. [[CrossRef](#)], [[Google Scholar](#)], [[Publisher](#)]
- [31] A. Moghimi, M. Abniki, *Adv. J. Chem. A*, **2021**, 4, 78-86. [[CrossRef](#)], [[Google Scholar](#)], [[Publisher](#)]
- [32] Y. Gao, M.G. Ierapetritou, F.J. Muzzio, *J. Pharma. Innov.*, **2013**, 8, 72-82. [[CrossRef](#)], [[Google Scholar](#)], [[Publisher](#)]
- [33] X. Manfei, D. Fralick, J.Z. Zheng, B. Wang, F. Changyong, *Shanghai Arch. Psychiatry*, **2017**, 29, 184. [[CrossRef](#)], [[Google Scholar](#)], [[Publisher](#)]
- [34] B. Guo, Y. Yuan, *Stat. Methods Med. Res.*, **2017**, 26, 1323-1340. [[CrossRef](#)], [[Google Scholar](#)], [[Publisher](#)]

HOW TO CITE THIS ARTICLE

Issam Mohammad Shakir, Bakr Sadiq Mohammed*, Nagham Shakir Turkey. A Novel Study in the Determination of Loratadine in Pharmaceutical Samples by Precipitating with 3,5-Dinitrosalicylic Acid Utilizing the NAG_4SX3_3D Analyzer at 0-180° in Conjunction with the Continuous Flow Injection Analysis (CFIA) Technique. *Adv. J. Chem. A*, 2024, 7(3), 260-277.

DOI: [10.48309/AJCA.2024.429274.1462](https://doi.org/10.48309/AJCA.2024.429274.1462)

URL: https://www.ajchem-a.com/article_189201.html